

Iron corrosion inhibition by olive mill wastewaters in acid medium

M. M. Rguiti^(a), M. Chadili^(a), B. El Ibrahimi^(a), A. Baddouh^(a), Lh. Bazzi^(b), M. Hilali^(a)
and L. Bazzi^{(a)*}

^(a) Applied Chemistry-Physic Team, Faculty of Sciences, IBN ZOHR University, Agadir. Morocco.

^(b) Autonomous Control Establishment and Coordination of Agadir Exports, Morocco

Abstract

In this paper, the effect of olive mill wastewater (OMW) as corrosion inhibitor for iron in molar hydrochloride solution was investigated by using potentiodynamic polarization (PDP) and electrochemical impedance spectroscopy (EIS) techniques. As results, both used techniques gave nearly the same efficiency of inhibition. Polarisation curves indicated that the OMW act as mixed inhibitor without variation of the hydrogen reduction mechanism. The inhibition efficiency increases by increasing OMW concentration to reach a maximum value of 84% at 4ppm. The effect of temperature on the corrosion of iron has also been studied without and with the inhibitor in the range from 298 to 318K. It was found that the rate of corrosion increases with temperature. OMW was adsorbed on the iron surface according to the model of the Langmuir adsorption isotherm.

* Corresponding author: :

l.bazzi@uiz.ac.ma

Received 18 Oct 2017,

Revised 12 Feb 2018,

Accepted 15 Feb 2018

Keywords: , inhibition, OMW, Iron, Hydrochloric acid

1. Introduction

Corrosion phenomena are defined as deterioration of the material by electrochemical or chemical reaction with the surrounding environment. It affects material properties such as mechanical strength, appearance, and permeability liquids and gases [1-4]. In fact, there are many methods of prevention and control of corrosion, among them the use of corrosion inhibitors which is very famous. Corrosion inhibitors are substances which, when added in small quantities in aggressive media, reduce or stop the reaction of the metal with the contact media. Organic inhibitors that contain nitrogen, oxygen and sulphur are more effective. In order to find an effective, environmental and economic inhibitor, researchers are directed to plant extras [5-24]. Since 1930, plant extracts have been used as natural corrosion inhibitors in acidic (H_2SO_4 , HCl ...) and basic media, for various metals such as iron, aluminium, stainless steel and its alloys. Several authors have shown that the inhibitory activity of plant extracts against corrosion is due to the existence of heterocyclic constituents such as phenolic compounds (tannins, flavonoids, etc.) [25]. Oil mill wastewater (OMW) is a liquid waste from the extraction of olive oil; it contains a large amount of organic matter (phenolic compounds, fatty acids, lipids and carbohydrates ...). In fact, in recent years, these effluents have received a great deal of attention for the presence of compounds with high added value, polyphenols which play the role of antioxidants, so they are used in the pharmaceutical and cosmetic field and also as food additives [26]. The objective of this study is to determine the potential using of oil mill wastewater (OMW) as corrosion inhibitor. The electrochemical techniques, namely: potentiodynamic polarization and impedance measurements are used to study the behaviour of iron in 1 M HCl solution in the absence and presence of the oil mill wastewater (OMW).

2. Material and Methods

2.1. Olive mill wastewaters sample

The olive mill wastewaters (OMW) samples used in this study was taken from a three-phase olive mill located in the region of *Essaouira* (the position of station is shown in fig.1)



Figure 1: The position in the olive oil extraction unit map where the OMW was collected.

The sample of OMW has been obtained from olives well ripened, collected in December 2016 and *stored* at 4°C . The effluent was subjected to several successive filtrations to remove the maximum suspended matter (TSS). The physical-chemical parameters of OMW were carried out in our laboratory according to the standard analytical methods for the examination of water and wastewater. The corresponding results are given in Table 1.

2.2. Chemicals

The aggressive solution (1mol/L HCl) was prepared by dilution of analytical grade 37% HCl with distilled water. Pure iron was used. Prior to all tests, iron electrode was prepared, by abrasive paper polishing up to 1200 degrees, and then rinsed with distilled water followed by acetone to remove fat matter.

Table 1: Physicochemical characterization of olive mill wastewaters (OMW) used in the corrosion tests

Parameters (unit)	Value
Turbidity (NTU)	2805
pH	5.22
conductivity (ms/cm)	10.52
DBO ₅ (g/L)	62
DCO (g/L)	180
K (g/L)	2.91
Na (g/l)	2.71
Cl(g/L)	3.37
Density(g/mL)	1.03

2.3. Electrochemical measurement

The electrochemical measurements were taken in a three conventional electrode Pyrex glass cylindrical cell. The working electrode (WE) is a rectangle iron plate. The surface exposed to the corrosive solution was 0.3 cm². A saturated calomel electrode (SCE) and a platinum electrode were used respectively as the reference electrode and the auxiliary electrode. To ensure reproducibility, all experiments were performed three times.

2.3.1. Polarisation measurements

The polarization curves are carried out using a Potentiostat /GalvanostatVersa STAT 3monitored by the VersaStudio software, with a sweep rate of 1 mV/s from – 800 to – 100 mV / SCE. The iron electrode was held at an open potential for 30 min. The inhibition efficiency **IE_p** (%) was determined by using the following relation:

$$IE_p(\%) = \frac{I_{corr} - I_{corr(inh)}}{I_{corr}} \times 100 \quad (1)$$

Where $I_{corr(inh)}$ and I_{corr} are the corrosion current densities of iron in the presence and absence of OMW, respectively.

2.3.1. EIS measurements

The electrochemical impedance spectroscopy (EIS) measurements were performed at the corrosion potentials (E_{corr}) after immersion in solution over a frequency range of 100 kHz to 10mHz with a wave amplitude of 10 mV by using the same electrochemical system. The inhibition efficiencies $E_{EIS}\%$ were calculated as follows [27]:

$$IE_{EIS}(\%) = \frac{R_{ct}(t) - R_{ct}(0)}{R_{ct}(t)} \times 100 \quad (2)$$

Where $R_{ct}(t)$ and $R_{ct}(0)$ are the polarisation resistances of iron in 1 M HCl solution with and without the additive, respectively.

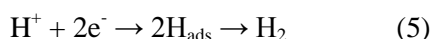
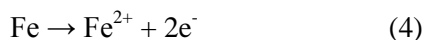
3. Results and discussion

3.1. Effect of concentration

3.1.1. Polarization curves

Potentiodynamic polarization curves of iron in 1 M HCl without and with different concentrations of the OMW inhibitor are represented respectively in figure 2. Table 2 gives the values of the associated electrochemical parameters. According to figure 2, it may be noted that the cathodic polarization curves gave rise to parallel Tafel lines

indicating that the hydrogen evolution is activation controlled and the reduction mechanism is not affected by the presence of OMW. The anodic reaction corresponds to the dissolution of iron as ferrous ions with the liberation of 2 electrons and the corresponding cathodic reaction has been reported to proceed as follows [28, 29]:



From the results obtained in Table 2, it is noted that the corrosion potential (E_{corr}) moves to the cathode sides. The classification of a compound as an anodic or cathodic inhibitor is achievable when the displacement of the corrosion potential is at least 85 mV compared to that measured for the virgin solution [30]. In our case the displacement was less than 14 mV. So we can classify our inhibitor as a mixed type inhibitor. From the results obtained in Table 2, it can also be noted that there is a decrease in the corrosion current densities when the concentration of the inhibitor has increased. The OMW inhibition efficiency reaches a maximum of 84% at 4 ppm.

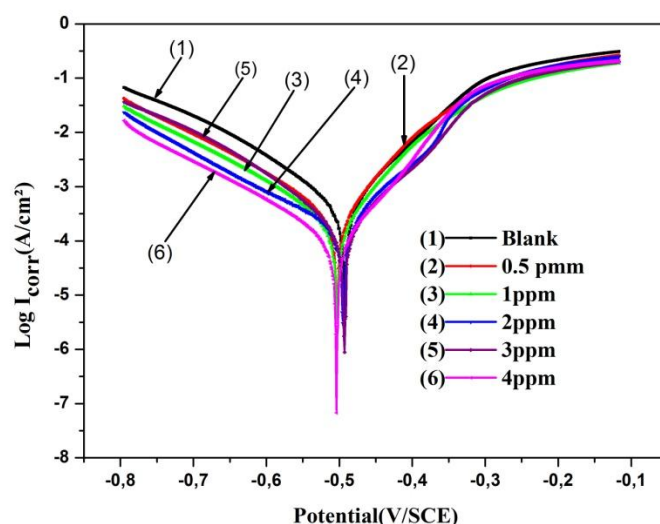


Figure 2: Polarisation curves of iron in 1M HCl without and with OMW at different concentrations.

Table 2: Electrochemical parameters of Iron at various concentrations of OMW in 1M HCl and corresponding inhibition efficiency.

OMW concentration	$-E_{\text{corr}}$ (mV)/SCE	b_a (mV dec ⁻¹)	b_c (mVdec ⁻¹)	I_{corr} ($\mu\text{A cm}^{-2}$)	IE_p (%)
Blank	493	81	121	477	-
0.5 ppm	504	68	124	300	37
1.0 ppm	518	67	124	208	56
2.0 ppm	496	70	118	175	63
3.0 ppm	494	69	125	121	75
4.0 ppm	505	66	117	77	84

3.1.2. Electrochemical impedances spectroscopy

The EIS plots for iron in the 1 M HCl solution in the absence and the presence of various concentrations of OWM are given in Fig. 3. The impedance parameters and the equivalent circuit model are given in Table 3 and Figure 4,

respectively. Overall, all experiments give us a single depressing loop, which is attributed to the dispersion of the frequency of the interfacial impedance [31, 32], generally due to the heterogeneity of the surface of the electrode. This heterogeneity may result from roughness, impurities, and dislocations, adsorption of the inhibitor and formation of porous layers [33, 34]. The equivalent circuit contains a constant phase element (CPE), in parallel with a resistor of charge transfer R_{ct} . This model has been described extensively in the literature [35-36]. The values of the CPE were calculated by using the equation (6):

$$Z_{CPE} = [Q(j\omega)^{-n}]^{-1} \quad (6)$$

The value of n allows us to differentiate the behaviour of an ideal capacitor ($n = 1$) and a CPE ($n < 1$). As cited previously, the values of I_{corr} decrease with the increase of the concentration of OMW. In this context, R_p it is inversely proportional to I_{corr} . As can be noted in the table 3, the values of R_{ct} increase with OMW concentration, which reaches a value of $337.2 \Omega cm^2$ at 4ppm, while the value of the CPE decreases [37]. Figure 5 shows the variation in the inhibitory efficiency as a function of the concentration of inhibitor, In fact the inhibitory efficiency, determined by potentiodynamic polarization as well as by electrochemical impedance spectroscopy, increases with the concentration of the inhibitor and averaged 84% at 4 ppm for a 30 min immersion time.

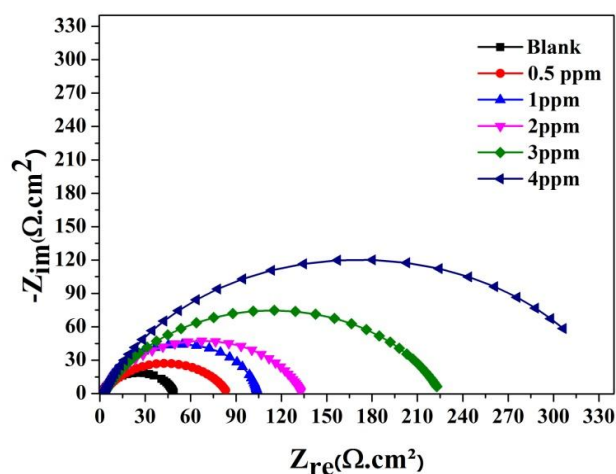


Figure 3: Nyquist plots of iron in 1M HCl solution without and with different concentrations of OMW.

Table 3: Impedance parameters of iron in 1M HCl solution containing different concentrations of OMW

Concentration	$R_s (\Omega m^2)$	$R_{ct} (\Omega cm^2)$	$CPE (S s^n cm^{-2})$	N	$IE_{EIS} (\%)$
Blank	1.9	48	6.50×10^{-4}	0.85	-
0.5ppm	2.6	82	4.94×10^{-4}	0.74	42
1.0 ppm	2.6	102	4.55×10^{-4}	0.91	53
2.0 ppm	2.8	130	3.51×10^{-4}	0.80	64
3.0ppm	2.8	223	3.20×10^{-4}	0.75	79
4.0ppm	2.7	337	1.50×10^{-4}	0.79	86

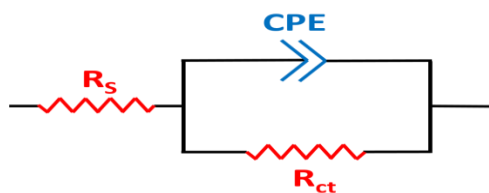


Figure 4: The used equivalent circuit to model the impedance spectra obtained for iron in different tested mediums.

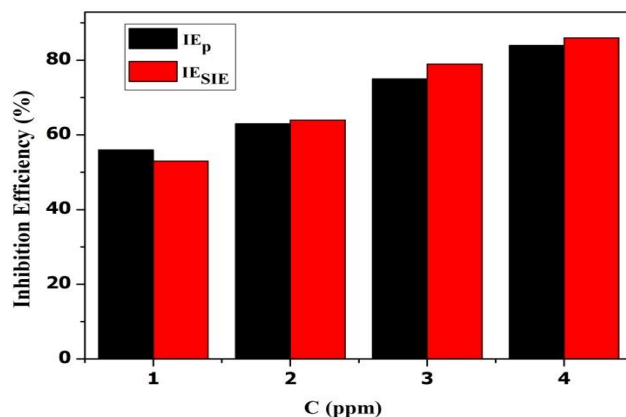


Figure 5: Variation of inhibition efficiency (IE %) with the concentration of OMW for iron in 1M HCl

3.2. Effect of temperature

3.2.1. Electrochemical polarisation

The nature of the environment and its temperature are two essential parameters affecting corrosion phenomena. In order to obtain an idea of the inhibition mechanism and to determine the activation energies of this process, the electrochemical measurements by polarization curves were taken at different temperatures in the absence and presence of the OMW at 4 ppm. Figure 6 shows the polarization curves of iron with and without 4 ppm of OMW at different temperatures. The corresponding data are shown in Table 4. We observed that corrosion rate increases with the temperature in the absence and in the presence of the OMW. However, the inhibition efficiency decreases slowly. It still important even at hay temperature (Table 4).

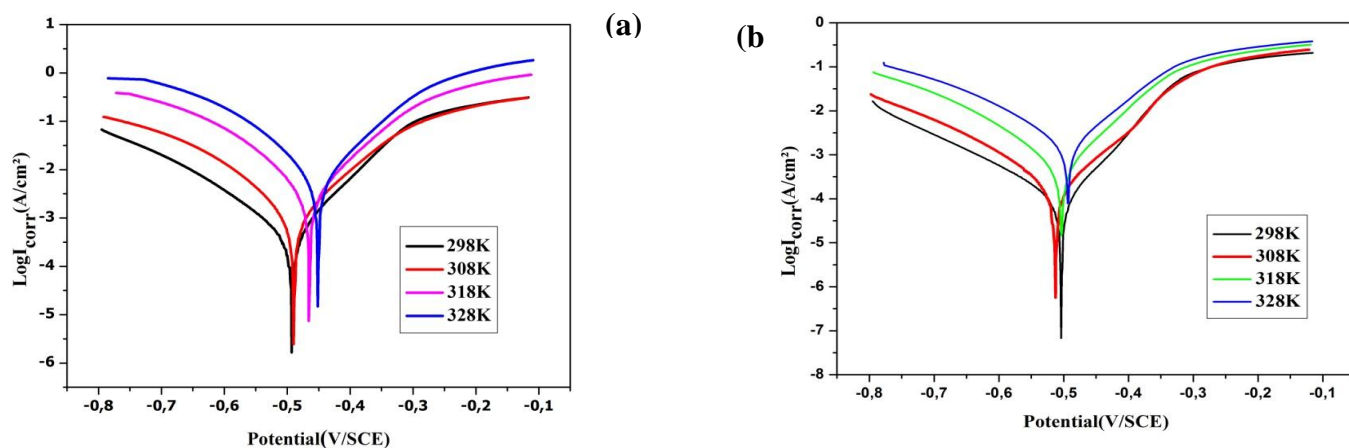


Figure 6: Effect of temperature on the cathodic and anodic responses for iron in 1 M HCl (a) and in 1M HCl + 4 ppm of OMW (b).

Table 4: Effect of temperature on iron in 1M HCl and with 4ppm of OMW

	T(K)	E_{corr} (mV)/SCE	I_{corr} ($\mu\text{A cm}^{-2}$)	$-b_c$ (mVdec ⁻¹)	b_a (mVdec ⁻¹)	IE _p (%)
Blank	298	496	477	121	81	-
	308	489	759	125	62	-
	318	464	2400	130	60	-
	328	452	4174	128	58	-
4ppm	298	505	77	126	66	84
	308	512	160	124	86	79
	318	503	580	123	80	76
	328	495	1341	117	82	68

3.2.1 Kinetic parameters

In order to get more information about the corrosion process, the activation kinetic parameters such as the activation energy (E_a), entropy (ΔS^*) and enthalpy (ΔH^*) are obtained from the effect of temperature using the Arrhenius law (Eq (6) and (7)) and the alternative formulation of the equation Arrhenius (Eq. (8) and (9)) [38-39]:

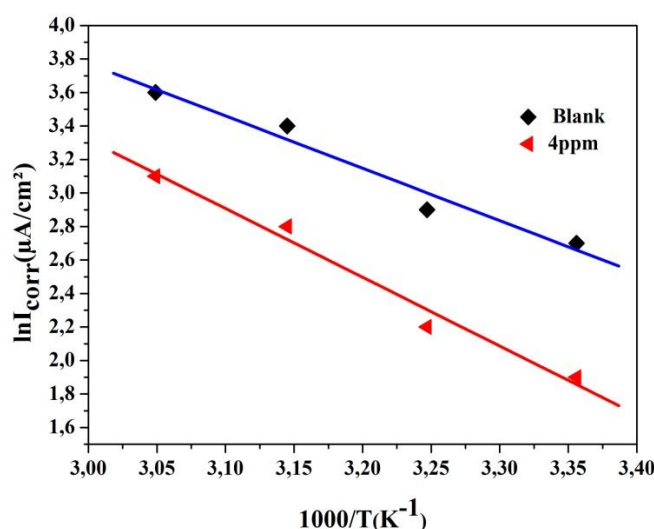
$$I_{corr} = A \exp\left(-\frac{E_a}{RT}\right) \quad (6)$$

$$\ln I_{corr} = \ln A - \frac{E_a}{RT} \quad (7)$$

$$I_{corr} = \frac{k_B T}{h} \exp\left(\frac{\Delta S^*}{R}\right) \exp\left(-\frac{\Delta H^*}{RT}\right) \quad (8)$$

$$\ln \frac{I_{corr}}{T} = A - \frac{\Delta H^*}{RT} \quad (9)$$

Where k_B : the Boltzmann constant ($k_B = 1.38066 \cdot 10^{-23} \text{ J K}^{-1}$), h : the Planck constant ($h = 6.6210 \cdot 10^{-34} \text{ Js}$).

**Figure 7:** Typical Arrhenius plots of iron in 1M HCl without and with addition of OMW at 4ppm

The variation of $\ln(I_{corr})$ as a function of $1000/T$ of iron in 1 M HCl without and with 4 ppm of OMW is presented in Figure 7. These curves show that the variation $\ln(I_{corr}) = f(1000/T)$ is substantially linear and follows the Arrhenius law both in the absence and presence of the inhibitor. The correlation coefficient (R^2) is 0.97. This result allowed us to calculate the activation energy values from the slope ($-E_a/R$). The variation of $\ln(I_{corr}/T)$ as a function of $1/T$ (Figure 8)

is a straight line with a slope $-\Delta H^*/R$ and an ordinate at the origin $\Delta S^*/R + \ln(kB/h)$ (Eq (9)) which used to determine the values of the activation parameters of the corrosion process: the enthalpy of activation ΔH^* and the activation entropy ΔS^* . As can be seen from table 5, the activation energy was higher in the presence of inhibitor compared to the blank solution that indicates the good performance of OMW inhibitor even at higher temperatures. This elevation of could be often interpreted as an indication for the formation of an adsorptive film by a physical mechanism [40-41].

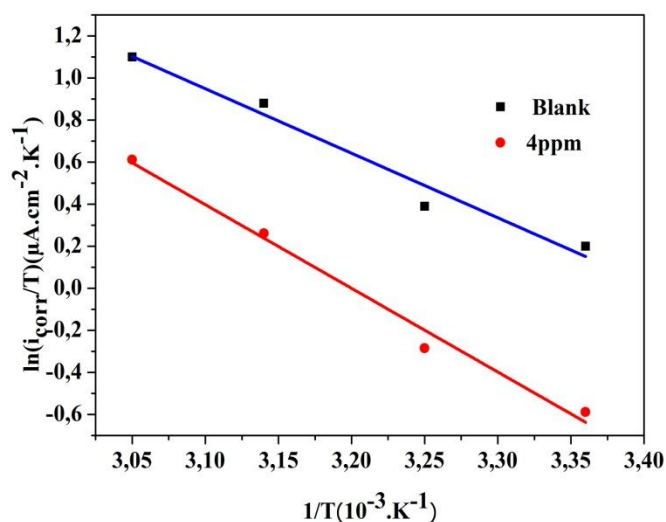


Figure 8: The relation between $\ln(I_{\text{corr}}/T)$ vs. $1/T$ for iron in 1M HCl without and with OMW at 4ppm.

Table5: Corrosion activation parameters of iron in 1 M HCl in absence and in presence of OMW at 4 ppm-

Medium	$\Delta H^*(\text{KJ.mol}^{-1})$	$\Delta S^*(\text{J.mol}^{-1}.\text{K}^{-1})$	$E_a(\text{KJ.mol}^{-1})$	$E_a - \Delta H^*$
Blank	23.4	-110.6	25.98	2.6
4 ppm	31.5	-91.7	34.10	2.6

3.3. Adsorption parameters

The adsorption depends on the charge of the metal, its nature, the chemical structure of the organic inhibitor and the type of electrolyte. The adsorption of the inhibitor can take place in two forms. The first is physical adsorption; it is a weak interaction which due to an electrostatic attraction between the molecules of inhibitor via charged atoms and the charged metal surface. The second form is chemical adsorption; it involves the transfer of charge from the adsorbate to the metal atoms to form coordination bonds. Chemical adsorption has activation energy higher than that of physical adsorption and therefore is generally irreversible [42-43]. In order to estimate the adsorption behaviour of the inhibitors there are various adsorption isotherms which can be used. To find the adsorption isotherm, the degree of surface coverage (θ) for several inhibitor concentrations was determined according to the following relationship:

$$\theta = \frac{EI(\%)}{100} \quad (10)$$

Table 6 gives the equations of tested isotherm model and corresponding linear correlation coefficients (R^2). It has been found that the Langmuir adsorption isotherm provides the best description of the adsorption behaviour of investigated inhibitor on iron surface in 1 M HCl solution, which gave a straight line with a unit slope. Recalling that the equation corresponding to the adsorption isotherm of Langmuir is represented below:

$$\frac{C_{inh}}{\theta} = \frac{1}{K_{ads}} + C_{inh} \quad (11)$$

Where K_{ads} is the adsorption/desorption equilibrium constant and C_{inh} is the ~~corrosion~~ inhibitor concentration in the solution. Therefore, the representation of $\frac{C_{inh}}{\theta}$ as a function of concentration C is presented on the Figure 10.

Table 6: Linear correlation coefficient of different tested adsorption isotherm models

Adsorption Isotherm	Equation	Linear correlation coefficient (R^2)
Freundlich	$Ln\theta = LnK + nLnC$	0.95
Temkin	$\theta = -\frac{1}{2a} LnK - \frac{1}{2a} LnC$	0.96
Langmuir	$\frac{C_{inh}}{\theta} = \frac{1}{K_{ads}} + C_{inh}$	0.99

The K_{ads} values can be calculated from the intercept lines on the C_{inh}/θ axis. This is related to the standard free energy of adsorption (ΔG_{ads}) by [44]:

$$K = 10^{-6} \exp\left(-\frac{\Delta G_{ads}}{RT}\right) \quad (12)$$

$$\Delta G_{ads} = -RT \ln(1.10^6 K_{ads}) \quad (13)$$

Where 10^6 is the concentration of water molecules expressed in $mg\ L^{-1}$, R is the universal gas constant and T is the temperature. In the present work, the calculated value of ΔG_{ads} is $-34.5 > -40.0\ KJ\ mol^{-1}$, on the one hand shows the stability of the adsorbed layer on the surface of the iron and the spontaneity of the adsorption process, on the other hand it support the mechanism of physical adsorption.

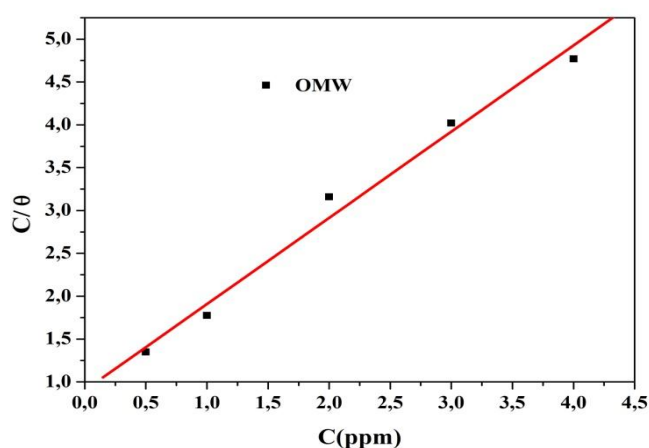


Figure 9: Langmuir isotherm adsorption model of OMW on the surface of iron in 1M HCl solution.

4. Conclusion

In this work, we have been able to avoid the OMW discharged into rivers and into the environment by using it as an effective corrosion inhibitor. Furthermore, this study has also brought the following results:

- OMW was a good inhibitor for iron in 1M HCl.
- The inhibition efficiency of OMW reached an optimum value of 84% at 4ppm.

- The inhibition efficiencies obtained by polarization curves and EIS are in good accordance.
- OMW acts as a mixed-type inhibitor without changing the hydrogen release mechanism.
- The adsorption of OMW on iron surface was found to be in agreement with Langmuir adsorption isotherm model. In addition, the calculated thermodynamic parameters such as K_{ads} and ΔG_{ads} indicated that the OMW adsorbed on to iron through physical mechanism.

References:

- [1] M.S. Al-Otaibi, A.M. Al-Mayouf, M. Khan, A.A. Mousa, S.A. Al-Mazroa, H.Z. Alkhatlan, S.A., Alkhatlan, H.Z., *Arabian Journal of Chemistry*, 7 (2012) 340-346.
- [2] I.B. Obot, N.O. Obi-Egbedi, *Corrosion Science*, 52 (2010) 198-204.
- [3] A. Yildirim, M. Çetin, *Corrosion Science*, 50 (2008) 155-165.
- [4] V. GENTIL, *Corrosão, Livros Técnicos e Científicos Editora*. (2003).
- [5] I.B. Obot, N.O. Obi-Egbedi, S.A. Umoren, *Corrosion Science*, 51 (2009) 1868-1875.
- [6] N.A. Negm, N.G. Kandile, E.A. Badr, M.A. Mohammed, *Corrosion Science*, 65 (2012) 94-103.
- [7] A.M. Abdel-Gaber, B.A. Abd-El-Nabey, E. Khamis, D.E. Abd-El-Khalek, *Desalination*, 278 (2011) 337-342.
- [8] M. Salasi, T. Shahrabi, E. Roayaei, M. Aliofkhazraei, *Materials Chemistry and Physics*, 104 (2007) 183-190.
- [9] G. Blustein, R. Romagnoli, J.A. Jaén, A.R. Di Sarli, B. del Amo, *Physicochemical and Engineering Aspects*, 290 (2006) 7-18.
- [10] P. Bommersbach, C. Alemany-Dumont, J.P. Millet, B. Normand, *Electrochimica Acta*, 51 (2005) 1076-1084.
- [11] A. Lecante, F. Robert, P.A. Blandinières, C. Roos, *Current Applied Physics*, 11 (2011) 714-724.
- [12] I. Radojčić, K. Berković, S. Kovač, J. Vorkapić-Furač, *Corrosion Science*, 50 (2008) 1498-1504.
- [13] P.C. Okafor, M.E. Ikpi, I.E. Uwah, E.E. Ebenso, U.J. Ekpe, S.A. Umoren, *Corrosion Science*, 50 (2008) 2310-2317.
- [14] M. Lagrenée, B. Mernari, M. Bouanis, M. Traisnel, F. Bentiss, *Corrosion Science*, 44 (2002) 573-588.
- [15] S. Kertit, J. Aride, A. Ben-Bachir, A. Sghiri, A. Elkholy, M. Etman, *Journal of Applied Electrochemistry*, 19 (1989) 83-89.
- [16] L. Wang, *Corrosion Science*, 43 (2001) 1637-1644.
- [17] M. Abdallah, H.E. Meghed, M. Sobhi, *Materials Chemistry and Physics*, 118 (2009) 111-117.
- [18] X.L. Cheng, H.Y. Ma, S.H. Chen, R. Yu, X. Chen, Z.M. Yao, *Corrosion Science*, 41 (1998) 321-333.
- [19] M.A. Hegazy, M. Abdallah, H. Ahmed, *Corrosion Science*, 52 (2010) 2897-2904.
- [20] S.S.A. El-Rehim, M.A.M. Ibrahim, K.F. Khaled, *Journal of Applied Electrochemistry*, 29 (1999) 593-599.
- [21] V.S. Sastri, *Corrosion inhibitors : principles and applications* / V.S. Sastri., Chichester ; New York : Wiley, c1998., 1998.
- [22] J.G.N. Thomas, *Ferrara*, Italy, 1980, University of Ferrara, 1980, pp. p 453. 414.
- [23] M.A. Quraishi, I. Ahamad, A.K. Singh, S.K. Shukla, B. Lal, V. Singh., *Materials Chemistry and Physics*, 112 (2008) 1035-1039.
- [24] S.K. Shukla, M.A. Quraishi, *Corrosion Science*, 51 (2009) 1007-1011.
- [25] P.B. Raja, M.G. Sethuraman, *Materials Letters*, 62 (2008) 113-116.
- [26] K.C. Emregül, O. Atakol, *Materials Chemistry and Physics*, 83 (2004) 373-379.
- [27] M.M. Solomon, S.A. Umoren, I.I. Udosoro, A.P. Udoh, *Corrosion Science*, 52 (2010) 1317-1325.
- [28] A. Aouniti, B. Hammouti, M. Brighli, S. Kertit, F. Berhili, S. El-Kadiri, A. Ramdani, *J. Chim. Phys.*, 93 (1996) 1262-1280.

- [29] H.B. Ouici, M. Belkhouda, O. Benali, R. Salghi, L. Bammou, A. Zarrouk, B. Hammouti, *Research on Chemical Intermediates*, 41 (2015) 4617-4634.
- [30] M.R. LAAMARI, J. BENZAKOUR., F. BERREKHIS., A. DERJA., D. VILLEMIN, D., *Les Technologies de Laboratoires*, 5(2010) 18-25.
- [31] S. Martinez, M. Metikoš-Huković, *Journal of Applied Electrochemistry*, 33 (2003) 1137-1142.
- [32] M. Elayyachy, A. El Idrissi, B. Hammouti, *Corrosion Science*, 48 (2006) 2470-2479.
- [33] A. Popova, E. Sokolova, S. Raicheva, M. Christov, *Corrosion Science*, 45 (2003) 33-58.
- [34] A.V. Benedeti, P.T.A. Sumodjo, K. Nobe, P.L. Cabot, W.G. Proud, *Electrochimica Acta*, 40 (1995) 2657-2668.
- [35] F. Mansfeld, *Corrosion*, 37 (1981) 301-307.
- [36] Z. Stoyanov, *Electrochimica Acta*, 35 (1990) 1493-1499.
- [37] R. Laamari, J. benzakoura, F. Berrekhisb, M. Bakassecc, D. Villemind, *J. Mater. Environ. Sci.*, 3 (2012) 485-496.
- [38] G. Trabanelli, M.E. F., *Corrosion Mechanism*, Marcel Dekker, (2006).
- [39] A.K. Singh, M.A. Quraishi, *Corrosion Science*, 52 (2010) 152-160.
- [40] A. Popova, E. Sokolova, S. Raicheva, M. Christov, *Corros. Sci.* 45 (2003) 33.
- [41] T. Szauer, A. Brandt, *Electrochim. Acta*; 22 (1981) 1209.
- [42] P. Roy, A. Pal, D. Sukul., *RSC Advances*, 4 (2014) 10607-10613.
- [43] A. Jmiai, B. El Ibrahimy, A. Tara, R. Oukhrib, S. El Issami, O. Jbara, L. Bazzi, M. Hilali, *Cellulose*, 24 (2017) 3843-3867.